Universal conductivity in the two-dimensional boson Hubbard model

G. G. Batrouni and B. Larson
Thinking Machines Corporation, 245 First Street, Cambridge, Massachusetts 02142

R. T. Scalettar
Physics Department, University of California, Davis, California 95616

J. Tobochnik
Physics Department, Kalamazoo College, Kalamazoo, Michigan 49006
and Physics Department, McGill University, Montreal, Québec, Canada H3A 2T8

J. Wang
Physics Department, McGill University, Montreal, Québec, Canada H3A 2T8
(Received 24 February 1993; revised manuscript received 24 May 1993)

We use quantum Monte Carlo methods to evaluate the conductivity σ of the two-dimensional disordered boson Hubbard model at the superfluid–Bose-glass phase boundary. At the critical point for particle density $\rho=0.5$, we find $\sigma_c=(0.45\pm0.07)\sigma_Q$, where $\sigma_Q=e_*^2/h$ from a finite-size scaling analysis of the superfluid density. We obtain $\sigma_c=(0.47\pm0.08)\sigma_Q$ from a direct calculation of the current-current correlation function. Simulations at the critical points for other particle densities, $\rho=0.75$ and 1.0, give similar values for σ. We discuss possible origins of the difference in this value from that recently obtained by other numerical approaches.

INTRODUCTION

The interplay between interactions and disorder has been a compelling field of research over the last decade. Particular interest has focused on two dimensions, both because randomness alone marginally localizes the eigenstates, and also because of a set of fascinating experiments on the superconducting-insulator transition.[1–6] These studies focused both on the possibility of a universal resistance with a value close to $h/4e^2=6.45$ kΩ, and also on the mechanism for the destruction of superconductivity.[7,8]

While the experiments tend to describe qualitatively similar behavior, the quantitative situation is still developing. Not only does the "universal conductance" in fact vary, but there can be nontrivial structure in the curves near the separatrix as the temperature is lowered. In particular, a "reentrant" phenomenon is observed in which the resistivity dips as if the film were about to go superconducting, but then the transition is usurped by the formation of an insulating state and the resistance rises as T is decreased further.[1] Further questions concern whether the experiments are really in the critical regime or not. That the experimentally accessible temperature ranges, $T\geq 0.5$ K, may not be sufficiently low is an issue that has been raised by, among other things, the existence of structure in the curves as T is reduced. This is a crucial question in determining the appropriate model for the critical phenomena, as we shall discuss further.

There have been a number of theoretical efforts to understand these phenomena.[9] A particularly interesting set of ideas has centered on the proposal that, despite the fact that the underlying degrees of freedom are fermionic, the appropriate model is one of disordered, interacting bosons,[9,10]

$$H=-\frac{t}{2}\sum_{\langle ij\rangle}(a_i^\dagger a_j+a_j^\dagger a_i)+\frac{V}{2}\sum_i n_i^2+\sum_i \epsilon_i n_i \ . \qquad (1)$$

Here $a_i^\dagger$ is a boson creation operator at site i, $n_i=a_i^\dagger a_i$ is the number operator, V is a soft-core on-site interaction, and ϵ_i is a random local chemical potential, which we chose to be uniformly distributed between $-\Delta$ and Δ. The physical motivation for a boson model is provided by imagining one has preformed Cooper pairs *above* the superconducting transition temperature, i.e., the fermions first condense into a set of interacting bosons that lack phase coherence. At lower temperatures phase coherence is established, and the system becomes superconducting. Such a view is particularly natural for granular systems where one can imagine Cooper pairs forming on individual grains. Cha *et al.*[11] have presented a more careful characterization of this general scenario by comparing correlation lengths for the various operator expectation values associated with the propagation of two electrons both together and independently. The fundamental physics is that, on the scale of the diverging pair-correlation length, Cooper pairs appear as point bosons.

However, the justification for considering the Hamiltonian equation (1) is by no means completely qualitative. The renormalization-group calculation of Giamarchi and Shultz[12] provides at least one explicit *theoretical* demonstration that the universality classes describing the superconducting transition of fermions with an attractive interaction and the superfluid transition for disordered bosons are identical. More detailed *experimental* justification of a picture of preformed bosons has been

provided by the work of Paalanen *et al.*,[13] which lends rather compelling support to a picture where the amplitude of the Cooper pair wave function is finite on both sides of T_c, and the superconducting transition is indeed described in terms of a loss of phase coherence between pairs rather than the breaking of the pairs themselves. Even so, it must be pointed out that tunneling experiments[8,14] on homogeneously disordered Pb films have indicated a vanishing of the gap at T_c. It therefore may be that granular and Josephson-junction systems are more appropriate realizations of bosonic models.

Here we will describe the results of quantum simulations combined with a finite-size scaling analysis to determine the conductivity at the superfluid-insulator transition in the boson-Hubbard model. The organization of this paper is as follows: We will first review briefly some of the analytic and numerical work to put our calculation in context. Next we describe our Monte Carlo method and discuss how the conductivity can be obtained either from a Kubo formula for the current-current correlation function, or, alternately, from the rigidity of the system to phase changes. We then detail our numerical results, beginning with the determination of the critical point for the Bose-glass–superfluid transition, and continuing with the analysis yielding the conductivity. The two techniques yield values which are the same to within our estimated error bars. However, this number differs substantially from that obtained previously.[15,16] We conclude with a discussion of some possible sources of this discrepancy.

Fisher *et al.*[10] have qualitatively mapped out the ground-state phase diagram of the boson-Hubbard model. In the clean limit, a gapless superfluid phase exists for all noninteger fillings. At commensurate densities, however, the interactions freeze the bosons into a gapped Mott insulating (MI) phase for sufficiently strong coupling. Increasing hybridization t will eventually wash out the gap and drive the system from insulator to superfluid. It was argued that this "coupling-driven" transition is in the universality class of the classical $(d+1)$-dimensional XY model. By contrast, changing the density away from an integer number of bosons per site can also induce superfluidity, but here the transition is mean field in character. When disorder is added, it was suggested[10] that a third, "Bose-glass," phase appears. This phase is characterized by the absence of a gap, but also by a vanishing superfluid density. While all noninteger boson densities were superfluid prior to the introduction of randomness, an incommensurate insulating phase is now possible as the disorder increases. This work[10,17] also predicted values or bounds for the critical exponents, some of which have been verified experimentally.[18]

The ground-state phase diagram was subsequently mapped out numerically[19–23] in one and two dimensions and also studied by the Bethe ansatz.[24] Quantitative values for the coupling required to localize the bosons into the MI phase were determined,[19,22,23] and the prediction of mean-field exponents for the density controlled transition was verified.[19] In the presence of disorder, the basic picture of the formation of a Bose-glass phase was substantiated, although a variety of unexpected reentrant phenomena were also observed.[20,22]

Numerical and analytic efforts have more recently turned to the transport properties for two-dimensional lattices, and, in particular, the evaluation of the conductivity. Runge used exact diagonalization techniques, combined with finite-size scaling, to extract the conductivity of the disordered, hard-core ($U=\infty$) model. He found $\sigma_c=(0.15\pm0.01)\sigma_Q$. In a set of papers,[11,16,25] the three-dimensional (3D) XY model and its Villain variant were studied with and without disorder and with short- and long-range potentials. It was argued that this model is in the same universality class as the disordered boson-Hubbard Hamiltonian. Cha *et al.*[11] obtained the conductivity first in the clean system with short-range interactions. The value $\sigma_c=(0.29\pm0.02)\sigma_Q$ found by Monte Carlo compared favorably with an analysis based on a $1/N$ expansion which gave $\sigma_c=0.251\sigma_Q$. Sorensen *et al.*[16] then showed that the addition of randomness results in a *smaller* value $\sigma_c=(0.14\pm0.01)\sigma_Q$, that is, farther from the experimentally realized numbers. Finally,[16] the disordered model with a long-range Coulomb potential was studied. Including these interactions was found to push the conductivity back up to $\sigma_c=(0.55\pm0.01)\sigma_Q$. This final value is certainly within a factor of 2 or so of the experiments, and possibly substantially closer especially considering uncertainties associated with the precise low-temperature experimental values.

None of these studies were of the Hamiltonian equation (1). It is of interest to compute the properties of the boson-Hubbard model directly, including the effect of the number fluctuations ignored in the mapping of the XY model and also in the hard-core diagonalization methods. One motivation is to test the arguments suggesting the universality classes are identical. In addition, if the experiments are not in the critical regime, then *nonuniversal* quantities become of interest, and the predictions of the original model are essential.

MONTE CARLO AND FINITE-SIZE SCALING METHODS

Here we present a brief discussion of our numerical approach. More detailed descriptions have recently appeared.[21,26] We begin by expressing the partition function as a path integral. In order to do this, we discretize the imaginary time $\beta=L_\tau\Delta\tau$ and use the Trotter approximation[27] to decompose the imaginary-time evolution operator.

$$Z=\mathrm{Tr}e^{-\beta H}=\mathrm{Tr}[e^{-\Delta\tau H}]^{L_\tau}\approx\mathrm{Tr}\left[\prod_i e^{-\Delta\tau H_i}\right]^{L_\tau}. \quad (2)$$

This is a well-controlled procedure since one can explicitly calculate at different $\Delta\tau$ and use well-understood techniques[28] to extrapolate to $\Delta\tau=0$. We now insert complete sets of states to express Z as a sum over a *classical* occupation number field $n(\boldsymbol{l},\tau)$:

$$Z=\sum_{\{n(l,\tau)\}}\langle n(l,1|e^{-\tau H_1}|n(l,2\rangle\langle n(l,2|e^{-\tau H_2}|n(l,3\rangle\cdots . \tag{3}$$

We have thus written our d-dimensional quantum-mechanical trace as a classical statistical mechanics problem in $d+1$ dimensions. The classical degrees of freedom to be sampled are the space imaginary-time-dependent boson occupation number field. Due to particle number conservation in H, the allowed configurations of this field trace out world lines as the particles propagate in τ. The "Boltzmann weight" of a particular configuration is the product of matrix elements, and can be sampled with standard stochastic techniques. Various choices are possible for the decomposition of H into H_i. We chose the "checkerboard" breakup in these studies.[29]

Expectation values are constructed in a similar way. Of particular interest to us will be the true (paramagnetic) current-current correlation function $\mathcal{J}^p_{xx}(\tau)$:

$$\begin{aligned}&\mathcal{J}^p_{xx}(\tau)=\langle j^p_x(\tau)j^p_x(0)\rangle\\&j^p_x(\tau)=e^{H\tau}j^p_x(0)e^{-H\tau},\\&j^p_x(0)=it\sum_i(a^\dagger_{i+\hat{x}}a_i-a^\dagger_i a_{i+\hat{x}}),\end{aligned} \tag{4}$$

and its Fourier transform

$$\mathcal{J}^p_{xx}(i\omega_m)=\int_0^\beta d\tau\langle j^p_x(\tau)j^p_x(0)\rangle e^{i\omega_m\tau}. \tag{5}$$

If we were able to evaluate these quantities at real frequencies, ω, we could then compute the frequency-dependent conductivity from the Kubo formula[30–32]

$$\sigma(\omega)=\sigma_Q\frac{2\pi}{\omega}[-\mathcal{J}^p_{xx}(\omega)-\langle k_x\rangle]. \tag{6}$$

Here k_x is the kinetic energy in one of the two equivalent lattice directions. The dc conductivity is then obtained from $\sigma_{dc}=\sigma(\omega\to 0)$. However, it is well known that the analytic continuation of quantities like the conductivity to real frequencies is a subtle problem.[33] Following Sorensen *et al.*,[16] our approach will be to exhibit that, for small Matsubara frequencies ($\omega_m=2m\pi/\beta$), the conductivity obeys $\sigma(i\omega_m)=\sigma_*/(1+|\omega_m|\tau_c)$. With the empirical observation that our data fit this analytic form, the continuation to $\sigma(\omega+i\delta)=\sigma_*/(1-i\omega\tau_c)$ is then possible. A direct calculation of σ, avoiding the assumption of the Drude form, similar to the computation of real frequency quantities in fermion simulations,[34] would be useful.

There is an alternate approach to obtaining the conductivity based, instead, on the response of the system to a phase twist. We define a "pseudocurrent" operator and its correlation function by

$$\tilde{\mathcal{J}}(\tau)=\frac{1}{\beta L^2}\sum_{\tau'}\langle\tilde{j}_x(\tau+\tau')\tilde{j}_x(\tau')+\tilde{j}_y(\tau+\tau')\tilde{j}_y(\tau')\rangle, \tag{7}$$

$$\tilde{j}_x(\tau)=\sum_{i=1}^{N_b}[x(i,\tau+1)-x(i,\tau)].$$

Here $x(i,\tau)$ is the x component of the position of boson i at time slice τ, N_b is the total number of bosons, and L the extent of the lattice in each spatial direction. Therefore, $\tilde{j}_x(\tau)$ measures the number of bosons moving in the positive x direction minus those moving the negative direction at time slice τ, i.e., the net boson flux per time step at time slice τ in the x direction. Similar definitions apply for the pseudocurrent in the y direction. This pseudocurrent operator was originally introduced[19] to measure the mean-square winding number and from that the superfluid density:[35]

$$\begin{aligned}&\tilde{\mathcal{J}}(\omega)=\sum_\tau e^{i\omega\tau}\tilde{\mathcal{J}}(\tau),\\&\tilde{\mathcal{J}}(\omega\to 0)=\frac{1}{\beta}\langle W^2\rangle,\\&\rho_s=\frac{1}{2t}\tilde{\mathcal{J}}(\omega\to 0).\end{aligned} \tag{8}$$

Defining $\rho_s(\omega)=\tilde{\mathcal{J}}(\omega)/2t$, we can show that the frequency-dependent conductivity can be written as

$$\frac{\sigma(\omega)}{\sigma_Q}=4\pi t\frac{\rho_s(\omega)}{\omega}. \tag{9}$$

Again a Drude form must be assumed here to carry out the analytic continuation.

Clearly, these two approaches are related, since they both yield the conductivity. Indeed, a detailed discussion of the connections between the response of the free energy to changes in the boundary conditions and the current-current correlation function has recently appeared.[32] However, despite these general relationships, the formulations of Eqs. (4)–(6) and (7)–(9) allow us to evaluate σ in two quite different ways. In particular, the current-current correlation function is a simple operator expectation value for the model described by the boson-Hubbard Hamiltonian. Meanwhile, the pseudocurrent analysis is based on topological properties of the boson world lines in our path-integral representation of the partition function. Thus, the two measurements serve as independent determinations of the conductivity and a check for the self-consistency of our simulations. However, we emphasize that such alternate numerical measurements, while yielding the same *average* value for the observable, can often exhibit rather different values of the *fluctuations* and even equilibration times. These possibilities are equally important motivations for considering both types of data.

It is useful to contrast our Monte Carlo approach with the two other numerical techniques already used in evaluating the conductivity. As discussed above, Runge[15] used an exact diagonalization method for the $U=\infty$ model. The advantage of that approach is, most importantly, that real-time correlation functions can be directly inferred, without the need for any analytic continuation. A second advantage is that there are no statistical errors from Monte Carlo sampling, only fluctuations associated with the disorder averaging. On the other hand, the technique is limited to rather small lattices (2×2 up to 5×5) since the Hilbert space dimension grows exponentially with the number of sites. Indeed, the Hilbert space

also grows rapidly with the number of bosons allowed per site, so that, in practice, it is necessary to consider the hard-core case where the site occupations are limited to 0,1. While this prevents the study of the transition as a function of interaction strength, as we will do, one is able to evaluate the conductivity for $U=\infty$ at a critical point accessed by changing the density.

Meanwhile, Monte Carlo simulations have also been conducted of a spin model (the classical 3D XY model) argued to be in the same universality class as the boson-Hubbard Hamiltonian. These studies are very close in spirit to the ones described here, since they are also simulations of a classical model in one higher dimension than the original quantum Hamiltonian. Unlike diagonalization, they are subject to error bars associated with statistical sampling and have to argue the analytic continuation, but they are able to study lattices of order 100 sites. There are two differences with our approach. The action in our simulation, the product of matrix elements of Eq. (3), is rigorously appropriate to the boson-Hubbard Hamiltonian. For example, the mapping to the spin-$\frac{1}{2}$ model neglects boson number fluctuations. Presumably, the advantage of the spin model approach is that the action is somewhat simpler than that arising from the quantum→classical world-line description detailed above. On the other hand, there are evidently assumptions associated with the universality class of the transition and the relevant degrees of freedom.

NUMERICAL RESULTS

In order to evaluate σ, we must first determine the superfluid-insulator critical point. Here we closely follow the finite-size scaling procedure of Ref. 16. According to two-parameter finite-size scaling, physical quantities, such as ρ_s, on different size lattices, of linear extent L, satisfy[36]

$$\rho_s = L^{\alpha} f(aL^{1/\nu}\delta, \beta L^{-z}) . \tag{10}$$

Here $\alpha=2-d-z$, β is the inverse temperature, and $\delta=(V-V_c)/V_c$ measures the distance to the critical point. The function f is universal but the metric factor a is not. The dynamic critical exponent z is predicted[37] to have the value $z=2$, and our system is two dimensional giving $\alpha=-2$. Notice that there is no nonuniversal metric factor for the second argument of the function f. Therefore, by keeping the second argument, βL^{-z}, fixed and plotting $L^2\rho_s$ versus V for different lattice sizes, all the curves should intersect at the critical value V_c. We chose the inverse temperature $\beta=(1/4)L^z\Delta\tau$ for different lattices L, i.e., the same aspect ratio as in Ref. 16. Data for $L^2\rho_s$, obtained from the pseudocurrent correlation function via the procedure described in Eqs. (7)–(9), is shown in Fig. 1. We see that the curves from different lattice sizes converge at a value $V/t\approx 7.0$. In order to resolve the critical point more accurately in Fig. 1, we need to improve the statistics by averaging over more realizations of disorder. To do that for many values of V takes a huge amount of computer time especially for the 12×12 system, and is therefore impractical. Instead, to

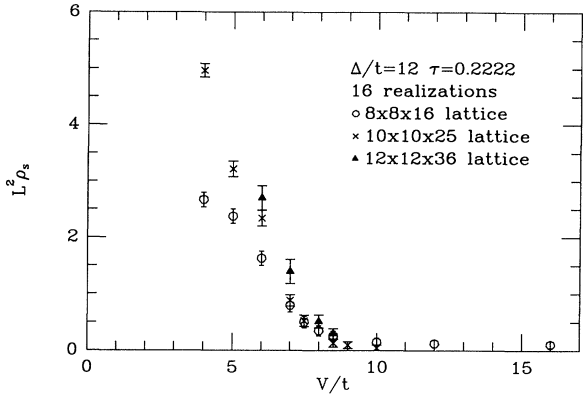

FIG. 1. The scaling variable ($L^2\rho_s$) vs the interaction strength V. The superfluid density ρ_s is obtained from the pseudocurrent correlation function via the procedure described in Eqs. (7) and (8). The convergence region of the different curves gives the approximate critical value for V.

make the simulation possible, we improved the statistics for the 8×8 and 10×10 systems and determined the crossing point of these two curves to be $V/t=7$. We then did high statistics runs for the 12×12 system at the value of V/t to ensure that, indeed, curves for larger systems will also intersect at the same point, thus giving $V_c/t=7$. To demonstrate the crossing of these curves we show $\rho_s(\omega)/\omega$ versus ω, for values from slightly below to slightly above the critical coupling, in Figs. 2(a)–2(c).

Figures 2(a)–2(c) show plots of $\rho(\omega)/\omega$ versus ω for different values of the coupling, $V/t=6.5, 7.0, 8.0$. We see that the best data collapse is at $V/t=7.0$. Furthermore, the plots show that the values 6.5 and 8.0 actually *bracket* the critical region. This is because for $V/t=6.5$ the data for $8\times 8\times 16$ lie slightly below those for $10\times 10\times 25$, as one would expect if the system is in the superconducting phase, while the pattern is reversed for $V/t=8.0$, as should happen when the system goes into the insulating phase. To obtain the conductivity, we fit the Monte Carlo data using $\sigma(\omega)=a/(1+b\omega_m)$ (solid lines in the figures). If we use the data for $V/t=6.5$ we find $\sigma\approx 0.5\sigma_Q$, whereas for $V/t=7.4$ (not shown) we get $\sigma=0.33\sigma_Q$. The best data collapse for $V/t=7.0$ gives $\sigma=0.4\sigma_Q$. To check the effect of the finite time-step errors, which are known to be $O(\Delta\tau^2)$, we redid the simulation for $V/t=7.0$, with the same β but twice as many time slices, i.e., half the $\Delta\tau$ as before. The results are shown in Fig. 3 and give $\sigma=0.44\sigma_Q$. Extrapolating to $\Delta\tau\to 0$ gives $\sigma/\sigma_Q=0.47\pm 0.08$.

In our simulations at half filling, $\rho=0.5$, the strength of the disorder was kept constant at $\Delta=6$, and the coupling, V, varied to find the critical point. The number of disorder realizations for most of our simulations is of the order of 100 (see the figures for more details). For the 8×8 and 10×10 lattices we did about 40 000 thermalization and 100 000 measurements sweeps, for the 12×12 lattice we did 100 000 thermalization and 20 000 measurement sweeps. We found that the large number of sweeps was necessary for thermalization and good statistics.

We now compute the conductivity from the true current-current correlation function using the Kubo relation by taking the limit $\sigma(\omega \to 0)$ in Eq. (9). In Fig. 4, we show the Fourier transform of the current-current correlation function, $\tilde{\mathcal{J}}(\omega)$, as a function of ω at the critical point $V=7.0$ for $\Delta=6$. For lattices sizes $N=8\times 8$, 10×10, 12×12. To obtain the conductivity, we fit the data with the Drude form

$$\tilde{\mathcal{J}}(\omega)-\tilde{\mathcal{J}}(\omega=0)=\frac{A\omega}{1+\omega T} . \tag{11}$$

According to the Kubo formula, Eq. (6), the kinetic energy should be subtracted from the frequency-dependent current-current correlation function to obtain the conductivity. Scalapino, White, and Zhang[31,32] demonstrated recently that whether or not the $q=0$ current-current correlations extrapolate to the kinetic energy k as $\omega \to 0$ can be used as a signature of the superfluid-insulator transition in the fermion Hubbard model. We have verified that this is true for bosons too because our independent measurements of the current and the kinetic energy do correctly signal this transition in agreement with other order parameters such as the superfluid density and gap. Indeed, this analysis provides a separate check on our code. Figure 5 is the same as Fig. 4 but with twice as many time slices.

Table I shows the values for the fitting parameters A and T, as well as the associated conductivity $2\pi A=0.38-0.46$ with the range in values representing changes due to different spatial and imaginary time lattice geometries. These numbers are in agreement to within our systematic and statistical uncertainties with those found from the independent analysis of the pseudo-

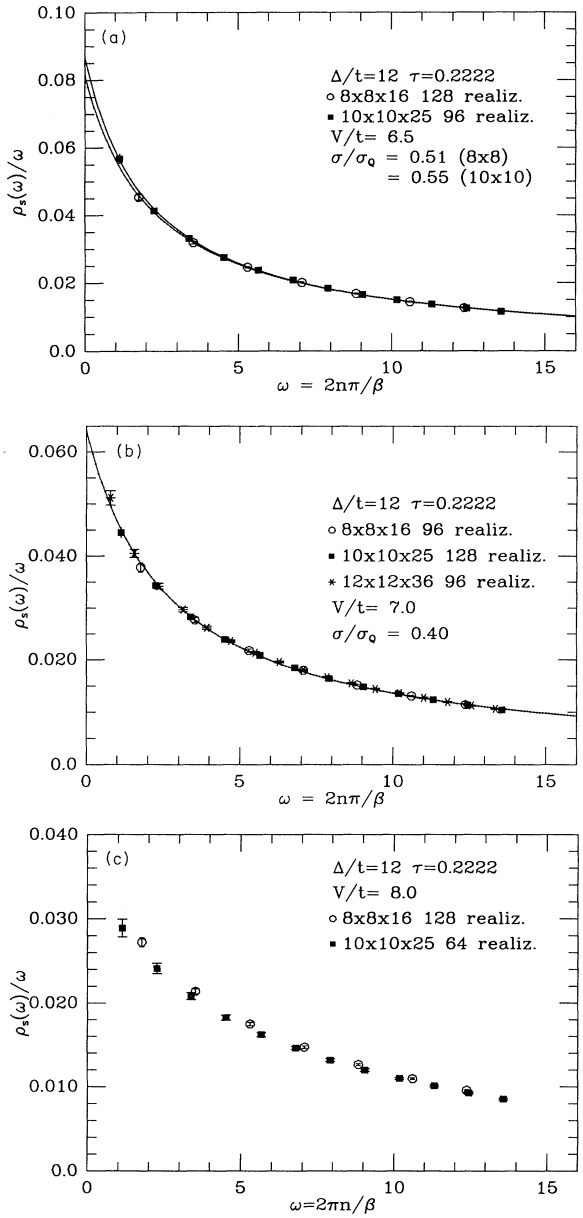

FIG. 2. Plots of $\rho_s(\omega)/\omega$ vs ω for different values of the coupling, $V/t=6.5, 7.0, 8.0$. The best data collapse indicates the critical point, and that happens for $V/t=7.0$.

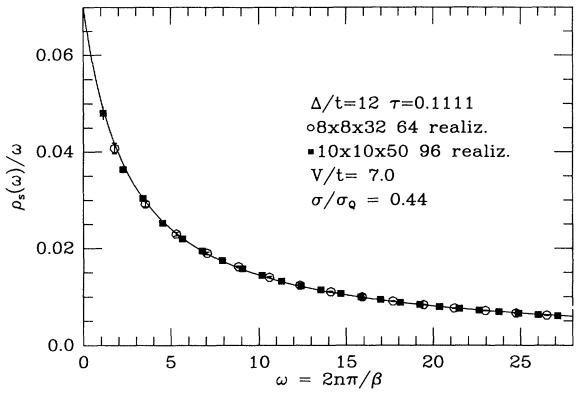

FIG. 3. Plot of $\rho_s(\omega)/\omega$ vs ω for coupling $V/t=7.0$. Here the number of time steps has been doubled to check for Trotter errors.

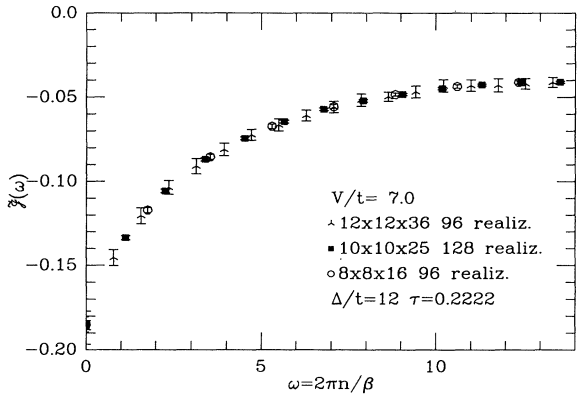

FIG. 4. $\tilde{\mathcal{J}}(\omega)$ as a function of ω at the critical point $V=3.5$ for $\Delta=6$ and lattice sizes $N=8\times 8$, 10×10, 12×12. The good data collapse again indicates that the system is at the critical point.

TABLE I. The values of the fitting parameters A and T used to obtain the smooth curves in Figs. 4(a)–4(c), and the associated number for the conductivity. A and T were obtained by fitting the analytic form Eq. (11) to the Monte Carlo data at $\omega=1$ and 2, a process which results in an excellent fit even out to much higher frequencies. The imaginary-time dimension has been chosen as $L=N^2/4$ for $\Delta\tau=\frac{2}{9}$ and chosen as $L=N^2/2$ for $\Delta\tau=\frac{1}{9}$, so that the inverse temperature β is the same for the two different discretization intervals. We have also done least-squares fits to the entire frequency range, a process which generally gave values for the conductivity which were higher by 10% or so. However, we believe that fitting to the low-frequency data is the more appropriate procedure, since the analytic form is expected to be most valid there.

N	$\Delta\tau$	A	T	σ
8×8	0.222	0.061	0.33	0.38
10×10	0.222	0.065	0.38	0.41
12×12	0.222	0.068	0.40	0.43
8×8	0.111	0.067	0.36	0.42
10×10	0.111	0.072	0.42	0.45

current in the previous section.

To check universality, we did similar simulations for $\rho=0.75$ and 1. The conductivity for $\rho=0.75$ near the transition is shown in Fig. 6. These results were obtained using simulations of 5000–20 000 sweeps for thermalization and 20 000–40 000 for averaging. Fifty realizations of the 8×8 lattice and 15 realizations of the 10×10 lattice were used. In these simulations $t\Delta/V$ was held fixed at $\frac{3}{7}$ while varying Δ and V/t. The transition was determined by searching for where the conductivity changes from increasing with size to decreasing with size, i.e., as in Figs. 2(a)–2(c). In the Bose-glass phase near the transition, we find that for the small lattices we are using it is difficult to distinguish between data which collapse on the same curve and data where the conductivity decreases with size. This may be one of the reasons why previous

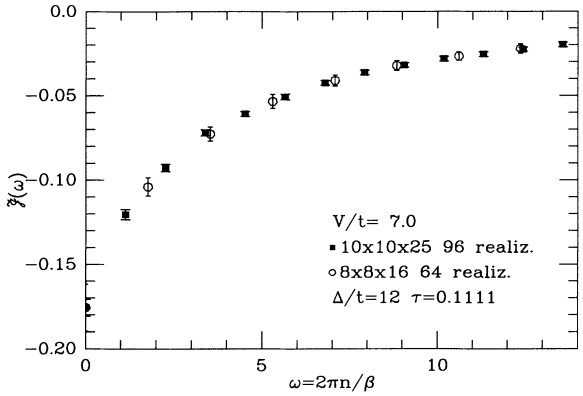

FIG. 5. $\mathcal{H}(\omega)$ as a function of ω at the critical point $V=3.5$ for $\Delta=6$, for lattice sizes $N=8\times8$, 10×10, 12×12. Here the number of time steps has been doubled (at fixed β) to check for Trotter errors.

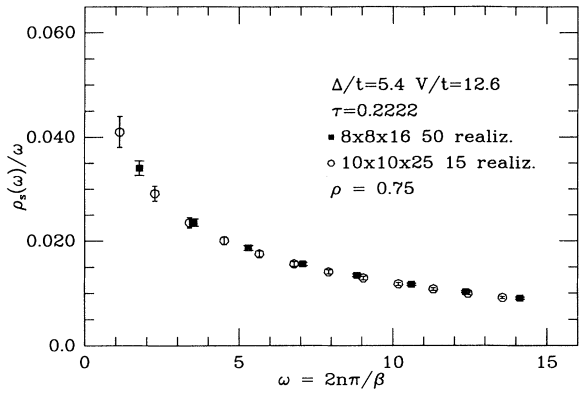

FIG. 6. Scaling plot as in Fig. 2 but at three-quarter filling. $\sigma/\sigma_q\approx0.37$.

studies have found lower values for σ. Fits of the data in Fig. 6 to the form $\sigma(\omega)=a/(1+b\omega_m)$ show that σ/σ_q varies from 0.36 to 0.38. The range of values depends on the number of data points used in the fit. Using all the data gives lower values; using only the two points closest to $\omega_m=0$ (which have larger statistical error bars) gives the higher values. At $\rho=1$ we obtain similar results as shown in Fig. 7. This is an important fact since it is possible that the Bose-glass phase would not completely cover the Mott lobe, and thus at integer filling one might find a phase transition from the superconductor directly into the Mott insulator. The data were obtained with 10 000 sweeps for thermalization and 40 000 sweeps for averaging. From 60 to 170 realizations were used for lattice sizes of $L=8$ and 10 and fixed $V/t=10$. These results show reasonable scaling. Again, estimates for σ/σ_q are in the range 0.3–0.4. The conductivity results for $\rho=0.75,1$ are consistent with those for $\rho=0.5$.

Our most accurate data are for half filling, and these were done on the Connection Machine CM5 with 32 and 64 processing nodes. The simulations for $\rho=0.75,1$ were done on Silicon Graphics work stations using a program written independently from the one used for half filling.

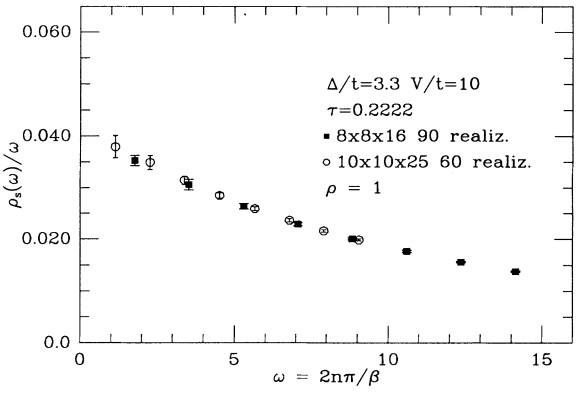

FIG. 7. Same as Fig. 6 but at $\rho=1$. $\sigma/\sigma_q\approx0.35$.

CONCLUSIONS

In this paper we have measured the conductivity of the disordered boson-Hubbard model. We obtain a value $\sigma = 0.46 \pm 0.08 \sigma_Q$ which differs from those previously reported for studies of a classical spin model[16] and diagonalization of hard-core boson systems on small lattices.[15] One possible source of this discrepancy is that we noticed in our data that the scaling curves which are extrapolated to zero frequency to obtain the conductivity are still curving upward toward large values for the larger lattices. It is therefore possible that for larger lattices than examined here (12×12) the conductivity could be even larger.

The precise source of this discrepancy is still under investigation. We believe that by evaluating the conductivity by two rather different approaches we have reduced the possibility of trivial questions of normalization. This still leaves the possibility of various numerical uncertainties, including questions concerning whether we average over a sufficient number of disorder realizations, the nature of Trotter errors, etc. We have examined this first point by dividing our 100+disorder realizations into groups of various sizes and comparing the averages and error bars from the different bins with each other. We did not observe phenomena like the averages disagreeing outside of error bars which would have been a signature of insufficient disorder averaging. We have explicitly checked the latter point by running at two values of $\Delta\tau$ and comparing the results. We found that this source of systematic error is small. We also carefully checked the equilibration of our lattice. The biggest source of uncertainty in our calculation is clearly in our determination of the critical point. From Fig. 2, it seems clear that our value for σ is rather sensitive to this choice, and a range of values is possible. However, we do not believe that the previously reported numbers are consistent with our data. This would require a choice of V_c clearly inconsistent with any sort of scaling plot. We are in the process of carrying out some exact diagonalization studies to pin down the source of the disagreement with QMC calculations.

ACKNOWLEDGMENTS

We would like to acknowledge useful conversations with A. Peter Young and Gergely Zimanyi. R.T.S.'s work was supported by National Science Foundation Grant No. NSF DMR-92-06023 and by the Donors of The Petroleum Research Fund, administered by the American Chemical Society. J.T. thanks the Physics Department at McGill University for its hospitality while on sabbatical and also acknowledges support from the Donors of The Petroleum Research Fund, administered by the American Chemical Society.

[1]B. G. Orr, H. M. Jaeger, A. M. Goldman, and C. G. Kuper, Phys. Rev. Lett. **56**, 378 (1986).
[2]D. B. Haviland, Y. Liu, and A. M. Goldman, Phys. Rev. Lett. **62**, 2180 (1989).
[3]H. M. Jaeger, D. N. Haviland, A. M. Goldman, and B. G. Orr, Phys. Rev. B **34**, 4920 (1986).
[4]S. J. Lee and J. B. Ketterson, Phys. Rev. Lett. **64**, 3078 (1990).
[5]A. F. Hebard and M. A. Paalanen, Phys. Rev. B **30**, 4063 (1984); Phys. Rev. Lett. **54**, 2155 (1985).
[6]L. G. Geerligs, M. Peters, L. E. M. de Groot, A. Verbruggen, and J. E. Mooij, Phys. Rev. Lett. **63**, 326 (1989).
[7]R. C. Dynes, J. P. Garno, G. B. Hertel, and T. P. Orlando, Phys. Rev. Lett. **53**, 2437 (1984); A. E. White, R. C. Dynes, and J. P. Garno, Phys. Rev. B **33**, 3549 (1986).
[8]R. C. Dynes, A. E. White, J. M. Graybeal, and J. P. Garno, Phys. Rev. Lett. **57**, 2195 (1986).
[9]For a brief review, see M. Cha, M. P. A. Fisher, S. M. Girvin, A. Wallin, and A. P. Yound, Phys. Rev. B. **44**, 6883 (1991), and the references cited therein.
[10]M. P. A. Fisher, P. B. Weichman, G. Grinstein, and D. S. Fisher, Phys. Rev. B **40**, 546 (1989).
[11]M. Cha, M. P. A. Fisher, S. M. Girvin, M. Wallin, and A. P. Young, Phys. Rev. B **44**, 6883 (1991).
[12]T. Giamarchi and H. J. Schulz, Phys. Rev. B **37**, 325 (1988).
[13]M. A. Paalanen, A. F. Hebard, and R. R. Ruel, Phys. Rev. Lett. **69**, 1604 (1992).
[14]J. M. Valles, R. C. Dynes, and J. P. Garno, Phys. Rev. B **40**, 6680 (1989).
[15]K. J. Runge, Phys. Rev. B **45**, 13 136 (1992).
[16]E. S. Sorensen, M. Wallin, S. M. Girvin, and A. P. Young, Phys. Rev. Lett. **69**, 828 (1992).
[17]M. P. A. Fisher, Phys. Rev. Lett. **65**, 923 (1990).
[18]A. F. Hebard and M. A. Paalanen, Phys. Rev. Lett. **65**, 927 (1990).
[19]G. G. Batrouni, R. T. Scalettar, and G. T. Zimanyi, Phys. Rev. Lett. **65**, 1765 (1990).
[20]R. T. Scalettar, G. G. Batrouni, and G. T. Zimanyi, Phys. Rev. Lett. **66**, 3144 (1991).
[21]G. G. Batrouni and R. T. Scalettar, Phys. Rev. B **46**, 9051 (1992).
[22]W. Krauth and N. Trivedi, Europhys. Lett. **14**, 627 (1991); N. Trivedi, D. M. Ceperley, and W. Krauth, Phys. Rev. Lett. **67**, 2307 (1991).
[23]K. G. Singh and D. S. Rokhsar, Phys. Rev. B **46**, 3002 (1992).
[24]W. Krauth, Phys. Rev. B **44**, 9772 (1991).
[25]S. M. Girvin, M. Wallin, E. S. Sorensen, and A. P. Young, Phys. Scr. **VT42**, 96 (1992); S. M. Girvin, M. Wallin, M. Cha, M. P. A. Fisher, and A. P. Young, Prog. Theor. Phys. Suppl. **N107**, 135 (1992).
[26]J. E. Hirsch, R. L. Sugar, D. J. Scalapino, and R. Blankenbecler, Phys. Rev. B **26**, 5033 (1982).
[27]H. F. Trotter, Proc. Am. Math. Soc. **10**, 545 (1959); M. Suzuki, Phys. Lett. **113A**, 299 (1985).
[28]R. M. Fye, Phys. Rev. B **33**, 6271 (1986); R. M. Fye and R. T. Scalettar, *ibid.* **36**, 3833 (1987).
[29]M. Barma and B. S. Shastry, Phys. Rev. B **18**, 3351 (1978). The two-dimensional version which we used in this study is discussed in M. S. Makivic and H.-Q. Ding, Phys. Rev. B **43**, 3562 (1991).
[30]G. D. Mahan, *Many-Particle Physics* (Plenum, New York,

1981).
[31]D. J. Scalapino, S. R. White, and S. C. Zhang, Phys. Rev. Lett. **68**, 2830 (1992), and the reference which follows, contain a detailed discussion of the issues involved in measuring the conductivity and superfluid density in numerical simulations.
[32]D. J. Scalapino, S. R. White, and S. C. Zhang (unpublished).
[33]J. E. Gubernatis, M. Jarrell, R. N. Silver, and D. S. Sivia, Phys. Rev. B **44**, 6011 (1991).
[34]R. N. Silver, J. E. Gubernatis, D. S. Sivia, and M. Jarrell, Phys. Rev. Lett. **65**, 496 (1990).
[35]E. L. Pollock and D. M. Ceperley, Phys. Rev. B **30**, 2555 (1984); D. M. Ceperley and E. L. Pollock, Phys. Rev. Lett. **56**, 351 (1986); E. L. Pollock and D. M. Ceperley, Phys. Rev. B **36**, 8343 (1987).
[36]V. Privman and M. E. Fisher, Phys. Rev. B **30**, 322 (1984).
[37]M. P. A. Fisher, G. Grinstein, and S. M. Girvin, Phys. Rev. Lett. **64**, 587 (1990).